Effects of Surfactants on Thermally Collapsed Poly(*N*-isopropylacrylamide) Macromolecules

Lay-Theng Lee*,† and Bernard Cabane‡

Laboratoire Léon Brillouin and Equipe mixte CEA-RP, SCM, CEA-Saclay, 91191 Gif sur Yvette, France

Received April 1, 1997; Revised Manuscript Received July 25, 1997[⊗]

ABSTRACT: Poly(*N*-isopropylacrylamide) macromolecules (PNIPAM) dissolve in water at temperatures below 33 °C; at higher temperatures, due to hydrophobic interactions, they precipitate out of solution. Addition of a small quantity of charged surfactant resolubilizes the precipitated polymer. We have used small angle neutron scattering to determine the structures of aqueous solutions of PNIPAM and sodium dodecyl sulfate (SDS). At temperatures above the precipitation temperature of the pure polymer solution, two different structures have been found, depending on the ratio of surfactant to polymer. At high ratios, SDS micelles bind to individual macromolecules and pull them into solution; the distance between consecutive micelles in a "necklace" is found to remain constant at around 60 Å. At low ratios, the macromolecules collapse to form small colloidal particles rather than forming necklaces with micelles spaced further apart. The collapse transition is abrupt in the sense that no intermediate states between the stretched necklaces and the collapsed colloidal particles have been found. A critical number of micelles per unit length of polymer is required for complete solubilization.

Introduction

Poly(*N*-isopropylacrylamide) (PNIPAM) is a water soluble polymer that precipitates out of water when the solution is heated above its cloud point of about 33 °C. It therefore exhibits an inverse solubility curve with a lower critical solution temperature (LCST), rather than an upper critical solution temperature compared to its counterpart polymers in organic solvents. This inverse behavior is neither novel nor unique to PNIPAM since most nonionic water soluble polymers that owe their solubility to hydrogen bonding (with water) also exhibit similar behavior. However, unlike poly(acrylamide) or poly(ethylene oxide), which have LCST values near or above the boiling point, the near ambient temperature of the LCST of PNIPAM makes it a very attractive candidate for the study of transitions of molecular structures, from coil to globule, and from hydrophilic to hydrophobic nature. For PNIPAM in water, this transition is found to be rather abrupt. The collapse transitions of PNIPAM chains in water and PNIPAM gels have been studied by Wu et al. for narrowly distributed high molecular weight samples.[1,2]

The practical applications of PNIPAM in its various forms, in different geometries and media and in different disciplines, can be found in a comprehensive review paper by Schild.[3] However, it is the relatively recent recognition of the transition of PNIPAM as a potential thermosensitive switching device that has prompted a surge in interest in the polymer, in both its native and modified forms. In some of its applications, additives are often present; surfactants are one such example. The presence of surfactants changes drastically the behavior of PNIPAM, most notably its solubility in water, and therefore the LCST. Extensive studies on the effects of anionic surfactants on the LCST of PNIPAM have been carried out by Schild and Tirrell.[4] Using surfactants of different chain lengths, these authors showed that the solubility of PNIPAM can be depressed or enhanced, depending on the alkyl chain length and concentration. Ricka et al.,[5] working under dilute solution conditions, proposed that redissolution of precipitated PNIPAM by surfactants proceeds in two distinct steps: intermolecular solubilization where isolated collapsed molecules are stabilized by surfactants, followed by intramolecular solubilization with increasing surfactant concentration. Other properties,[6,7] including characterization of the phase behavior using light scattering,[8] as well as rheological behavior[9] of PNIPAM−surfactant systems have also been investigated.

In spite of the copious amount of work that has already been done to understand the physico-chemistry properties of PNIPAM−surfactant interactions, little information obtained from direct measurements exists regarding the structural properties of the polymer−surfactant complexes. Our present work addresses this latter aspect. In this paper, we report small angle neutron scattering data of semidilute solutions of PNIPAM in the presence of sodium dodecyl sulfate at temperatures below and above the LCST. In this technique, the possibility to vary the contrast of the different scattering objects by isotopic substitution allows us to study separately the structures of the polymer and the surfactants.

Experimental Section

Materials and Polymer Synthesis. *N*-Isopropylacrylamide monomer from Eastman Kodak Co. was recrystallized in a mixture of hexane and benzene. After three cycles of degassing through freezing and thawing, polymerization was carried out in benzene by the free radical polymerization method at 50 °C using azobis(isobutyronitrile) (AIBN) as initator (from Alfa Chemical and used as received). The polymerized material was dissolved in acetone and precipitated in hexane. This methodology was adopted from the paper of Schild and Tirrell.[4] The molecular weight of the polymer determined by size exclusion chromatrography coupled with low angle light scattering is $M_w = 1.05 \times 10^6$ with a polydispersity index $I_p = 2.0$.

Scattering Techniques. Contrasts.[10] The small angle scattering of neutrons originates from the spatial variations in the sample of a quantity that is related to the index of refraction for neutrons. This quantity is the scattering length density, ρ, which is calculated by summing the scattering

† Laboratoire Léon Brillouin.
‡ Equipe mixte CEA-RP, SCM.
[⊗] Abstract published in *Advance ACS Abstracts,* September 15, 1997.

S0024-9297(97)00446-4 CCC: $14.00

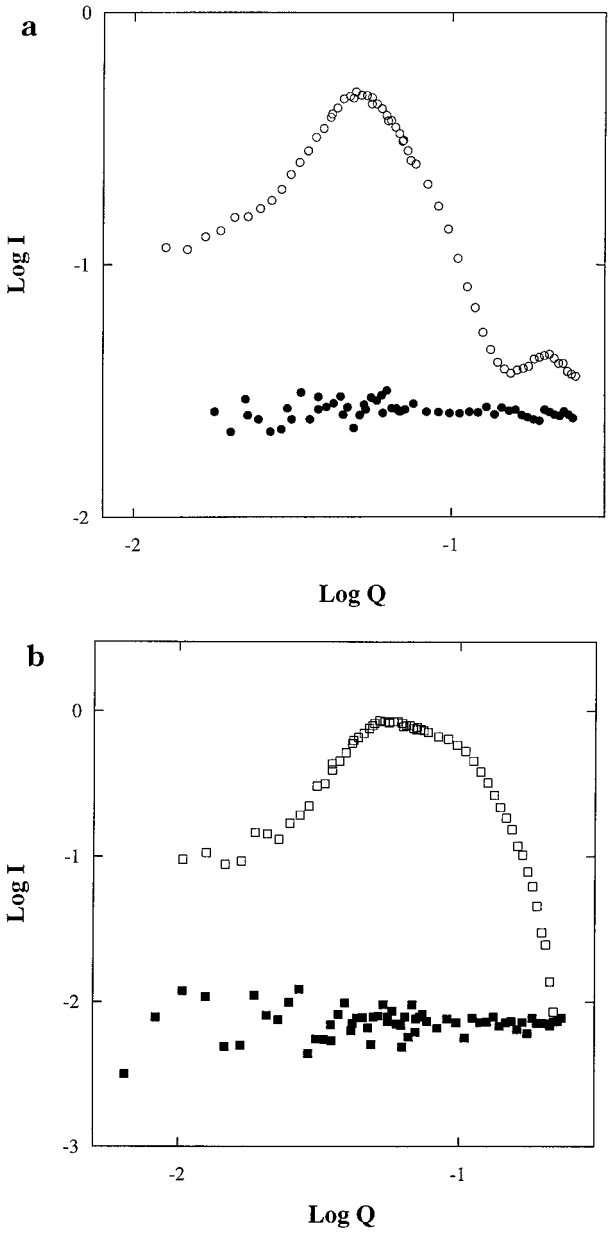

Figure 1. (a) Scattering curves of protonated PNIPAM and deuterated SDS in D_2O at $C_p = C_s = 0.03$ g/mL at $T = 20$ °C: (open circles) PNIPAM + deuterated SDS; (closed circles) deuterated SDS alone. (b) Scattering curves of protonated PNIPAM and deuterated SDS in a 20% D_2O/80% H_2O volume mixture at $C_p = C_s = 0.03$ g/mL at $T = 20$ °C: (open squares) PNIPAM + deuterated SDS; (closed squares) PNIPAM alone.

lengths of individual nuclei per unit volume. In aqueous solutions, the intensities scattered by different solutes are proportional to the square of the difference, $\Delta\rho$, between their scattering length densities and that of water. With organic solutes, the differences are usually small, unless isotopic substitution of H by D is used. Replacing H_2O by D_2O or protonated molecules by deuterated ones leads to large differences in $\Delta\rho$.

In this work, we discuss two types of scattering: scattering from polymer and scattering from surfactant. In *scattering from polymer*, protonated PNIPAM, deuterated SDS, and pure D_2O are used. Deuterated SDS is nearly contrast-matched to pure D_2O; therefore, scattering from the surfactant is suppressed and the resulting scattering signal is mostly from the polymer molecules (Figure 1a). In *scattering from surfactant*, protonated PNIPAM, deuterated SDS, and a 20% D_2O/80% H_2O volume mixture are used. In this mixture, the PNIPAM molecules are almost contrast-matched to the solvent and scattering is predominantly due to the surfactant molecules (Figure 1b).

We point out that isotopic substitution may produce nonnegligible effects in some systems due to a difference in the interaction parameters of deuterium and hydrogen, resulting in a modification of the phase transition behavior. For a PNIPAM solution of $C_p = 0.002$ g/mL, we found LCST values of 33.1 and 33.9 °C in H_2O and D_2O, respectively. Our present studies are carried out at temperatures far from the LCST, 20 and 40 °C, where the PNIPAM molecules are without doubt either in good solvent condition or in a collapsed state. Therefore the effect of isotopic substitution on the collapse transition of the polymer does not have any important consequences on our interpretation of the data. Furthermore, it has been found that isotopic substitution does not alter the SDS micellar structure.[11]

Scattering Curves. The scattering curves result from interferences between neutron rays scattered by different nuclei in the sample. The interferences are determined by the scalar product $\mathbf{Q}\cdot\mathbf{r}$, where $\mathbf{Q}$ is the scattering vector and $\mathbf{r}$ is the vector separating points. For isotropic samples, only the magnitude Q of the scattering vector matters, which is determined by the wavelength λ of incident neutrons and the scattering angle θ:

$$Q = (4\pi/\lambda)\sin(\theta/2) \tag{1}$$

Then the scattering pattern may be reduced to a scattering curve $I(Q)$. From this scattering curve, some geometrical parameters that characterize the distribution of scattering length in the sample may be determined. The description is easiest when the sample is a dispersion of identical, uncorrelated objects, because interferences between objects cancel out, and only interferences within each object need to be considered.

Dispersions of Identical Uncorrelated Objects.[10,12] At $Q = 0$, all rays are in phase, and the scattered intensity measures the content of each object, as expressed by its volume V and the difference in scattering length density, $\Delta\rho$:

$$I_0 = KNV^2(\Delta\rho)^2 \tag{2}$$

where K is an instrumental constant and N is the number of uncorrelated objects. Thus, the volume V per object or the corresponding mass can be extracted from the absolute value of I_0. Alternatively, instead of determining the instrumental constant K, it is possible to normalize I_0 by the integral of the intensity scattered in all directions. Accordingly, the dry volume per particle can be calculated as

$$V = \frac{I(Q\rightarrow 0)}{(1/2\pi^2)\int Q^2 I(Q)\,\mathrm{d}Q} \tag{3}$$

At low Q, the intensity decays because of interferences between rays scattered by points located at opposite ends of each object. The decay is related to the radius of gyration R_g of the object through the Guinier law:

$$I(Q\rightarrow 0) = I_0(1 - Q^2R_g^2/3) \tag{4}$$

At intermediate Q values, the intensity decays faster, because all rays scattered by each object interfere destructively. The rate of the decay depends on the shape of the object: rodlike objects give a Q^{-1} decay, flat objects such as disks or shells give Q^{-2}, and dense globules follow Porod's law, which is Q^{-4}. The precise shape of the scattering curves may be calculated for objects that have a simple geometry. For homogeneous spheres of outer radius R, where $R = 1/\sqrt{0.6}R_g$, the scattering curve is a function that starts according to eq 2 and then oscillates around the Q^{-4} decay of Porod's law. For spherical shells, the scattering curve has a similar shape, but its asymptotic behavior is a Q^{-2} decay.

Dispersions of Correlated Objects.[13,14] If the positions of the objects in the dispersion are not completely random, the interferences between rays scattered by neighboring objects do not cancel out, and the intensity is modified by these interferences. For concentrated dispersions of identical, spheri-

cal objects, the intensity can be expressed as:

$$I(Q) = I_1(Q)\, S(Q) \tag{5}$$

where $I_1(Q)$ is the intensity of noncorrelated objects and $S(Q)$ is the structure factor that describes the correlations. $S(Q)$ is a Fourier transform of the pair correlation function of the dispersion. For repelling objects, such as surfactant micelles, $S(Q)$ is depressed at low Q because long wavelength fluctuations of the number density of micelles are suppressed by the repulsions; it has a peak at a Q value corresponding to the most probable intermicellar distance d ($Q = 2\pi/d$), and it oscillates back to unity at higher Q values.

The scattering from micelles has been extensively studied. From the shape of the peak in the intensity, it is possible to calculate the parameters that determine the structure of the micellar solution, i.e., the micelle size and shape and the strength of intermicellar repulsions.

Instruments. Scattering experiments were performed on the instruments PAXE at LLB, Saclay, and D22 at ILL, Grenoble. The data were collected on an XY detector and radially averaged. Subsequently, background spectra were subtracted from sample spectra, and spectra obtained at different detector positions were grouped in a single file. All intensities were normalized by the intensity of a standard scatterer; this allows a comparison of intensities scattered by samples containing different amounts of polymer or surfactant.

Results and Structural Analysis

At $T = 40$ °C, water is a nonsolvent for the polymer. At this temperature, samples with low ratios of surfactant to polymer are turbid dispersions, whereas samples with higher ratios are clear solutions. We present scattering curves from samples prepared at fixed polymer concentration, C_p (either 10^{-2} or 3×10^{-2} g/mL) and increasing surfactant/polymer ratio, S/P. For S/P = 0, the sample is macroscopically phase separated; for S/P = 0.01−0.3, the solutions are turbid, and for S/P = 0.4−2, the solutions are clear.

At $T = 20$ °C, water is a good solvent for the polymer, and all samples are clear solutions. We present also scattering curves for the same samples.

Temperature $T = 40$ °C. S/P = 0 and 0.05. These samples are macroscopically phase separated: a white solid containing all the polymer coexists with excess aqueous solution. The scattering curve of the polymer shows a very high intensity in the $Q \rightarrow 0$ limit, and then a Q^{-4} decay over the whole range of Q values (Figure 2). This is in line with the scattering expected from macroscopic pieces of a dense polymer phase, with sharp boundaries, in agreement with the visual appearance of the samples. The scattering from the surfactant is quite weak, because the surfactant concentration is extremely low.

S/P = 0.15, 0.2, and 0.3. These samples are turbid, visually homogeneous dispersions. *The scattering curve of the polymer* starts at low Q with a flat section, at relatively high intensity; then it curves downward and continues with a Q^{-4} decay (Figure 2). This part of the scattering curve matches the scattering expected from *colloidal particles*. From the value of the intensity scattered at $Q \rightarrow 0$, the average dry volume per particle was calculated according to eq 3. At S/P = 0.15, 0.20, and 0.30, the calculated volumes are $V = 1.26 \times 10^8$, 1.21×10^8, and 8.8×10^7 Å^3, respectively, corresponding to dry radii $R_v = 294$, 290, and 261 Å. From the curvature of the scattering curve at low Q, the values of R_g calculated according to eq 4 for these surfactant concentrations are 298, 294, and 269 Å, giving corresponding outer radii $R = 385$, 379, and 347 Å. The radii extracted from R_g are larger than the values of R_v because they reflect different moments of a broad distribution of particle sizes. Indeed, when a Schultz size distribution expression[15] for polydisperse homogeneous spheres is fitted to these data, the mean radii, $\bar{R}$, obtained are 212, 208, and 185 Å, respectively, with a width parameter $z = 5$, where $(z + 1)^{-1/2} = (\overline{R^2} - \bar{R}^2)^{1/2}/\bar{R}$.

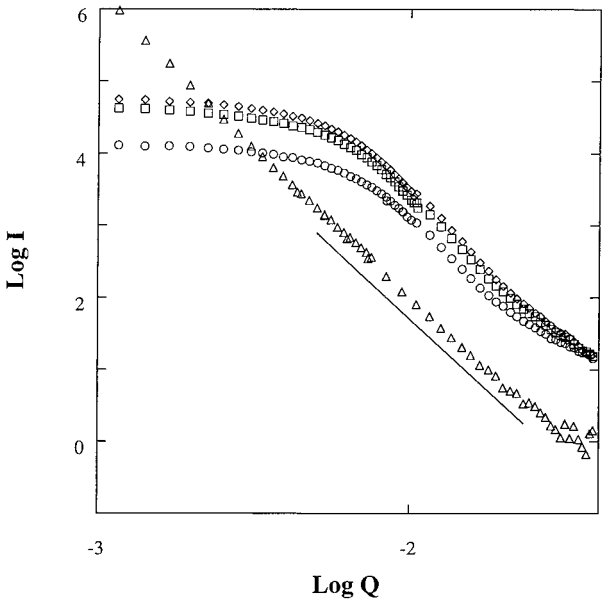

Figure 2. Scattering from polymer in samples with low S/P, $C_p = 0.01$ g/mL and $T = 40$ °C: (triangles) S/P = 0 (macroscopically separated); (diamonds) S/P = 0.15 (turbid); (squares) S/P = 0.2 (turbid); (circles) S/P = 0.3 (turbid). The continuous line has a slope of −4.

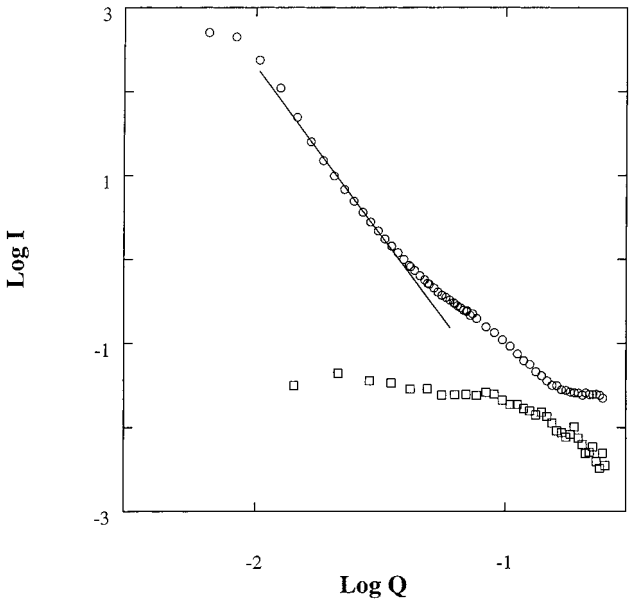

Figure 3. Scattering from samples with $C_p = 0.03$ g/mL and S/P = 0.1 at $T = 40$ °C (turbid): (circles) scattering from polymer; (squares) scattering from surfactant. The continuous line has a slope of −4.

At higher Q, the scattered intensity is slightly above the Q^{-4} law that would be expected for spheres with sharp boundaries (Figure 3). In this Q range and for all the following data, C_p was increased to 0.03 g/mL in order to increase the scattering signal. This excess intensity could originate from partially solubilized chains forming a hairy layer around the colloidal

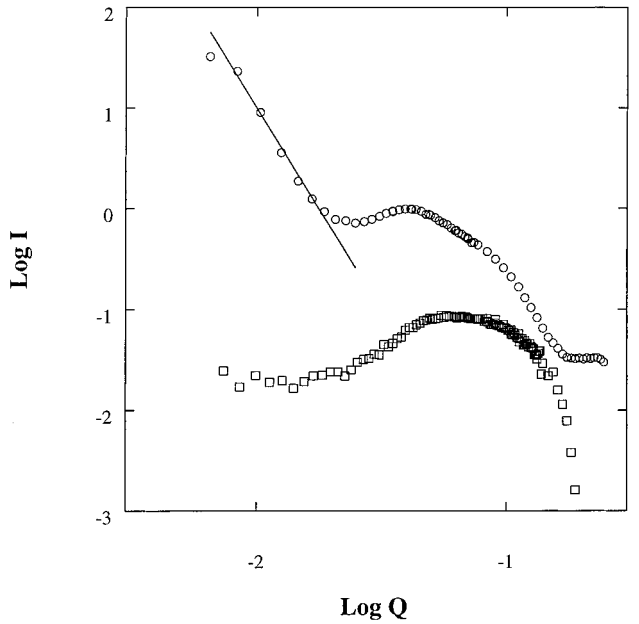

Figure 4. Scattering from samples with $C_p = 0.03$ g/mL and S/P = 0.3 at $T = 40$ °C (turbid): (circles) scattering from polymer; (squares) scattering from surfactant. The continuous line has a slope of −4.

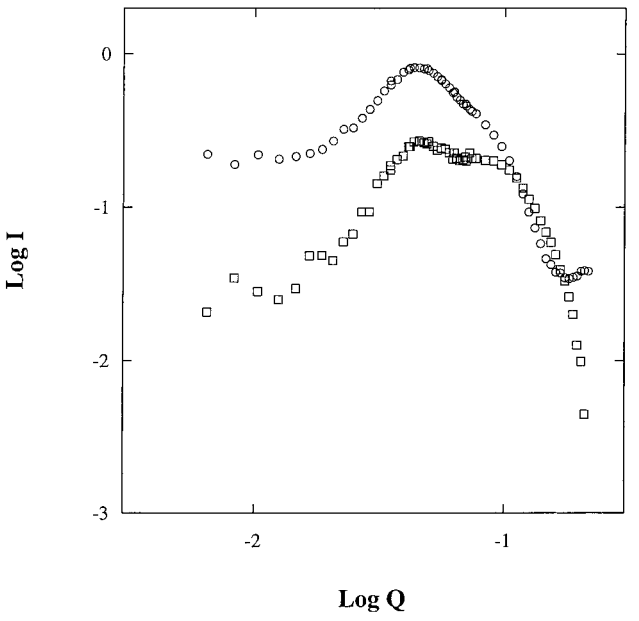

Figure 5. Scattering from samples with $C_p = 0.03$ g/mL and S/P = 0.5 at $T = 40$ °C (clear solution): (circles) scattering from polymer; (squares) scattering from surfactant.

particles or from fully dissolved chains that are pulled into solution and coexist with the colloidal particles.

The *scattering of the surfactant* is still weak; it shows a slow decay followed by a plateau and, beyond $Q = 0.1$ Å^{-1}, a steeper decay (Figure 3). The real space distance that marks the right edge of the plateau is $d = 63$ Å. This scattering is *not* what would be expected for surfactant bound to the polymer particles. Indeed, surfactant forming shells around the particles would give a strong scattering at low Q, followed by a Q^{-2} decay. Instead, the observed slow decay and plateau could originate from surfactant micelles bound to dissolved macromolecules. This would indeed yield a slow decay followed by a shoulder at the intermicellar spacing, in agreement with the observed scattering reported by Cabane and Duplessix.[16]

At S/P = 0.3, the *polymer scattering* is still high at low Q (Figure 2). The plateau, the downward curvature, and the following Q^{-4} decay attest the presence of *colloidal particles*. However, the decay is interrupted by a peak located at $Q = 4.2 \times 10^{-2}$ Å^{-1}, corresponding to a real space distance of $\xi = 150$ Å (Figure 4). Finally, at very high Q, the scattering curve has an oscillation corresponding to a real space distance $h = 32$ Å. The scattering at high Q remains much above the continuation of the Q^{-4} decay, indicating that a substantial fraction of the polymer is not in the colloids. All this excess scattering (i.e., scattering that is in excess of the Q^{-4} decay) demonstrates the coexistence of dissolved macromolecules with the polymer that is in the colloidal particles.

The *surfactant scattering* is still weak; nevertheless, it shows two interesting features: (i) a peak located at the same Q value as the polymer peak (real space distance $\xi = 150$ Å) and (ii) a second peak located at higher Q (real space $d = 63$ Å). Feature (i) matches that in the polymer scattering curve; therefore *the surfactant must be associated with the dissolved polymer*.

S/P = 0.4−1.0. These samples are clear solutions. The *polymer scattering* is depressed at all Q values below 3×10^{-2} Å^{-1}, and then it has a strong peak located at a real space distance $\xi = 141$ Å for S/P = 0.5 (Figure 5). In comparison with the spectra of the sample at S/P = 0.3, the main difference is the suppression of the strong scattering at low Q that was caused by the polymer particles. This is consistent with the transparency of the solutions. Thus, a certain amount of surfactant (S/P = 0.4) *causes complete dissolution of the polymer particles*. Moreover, the depression and peak are characteristic of small repelling objects;[17] the characteristic distance ($\xi = 141$ Å) is close to what would be calculated for a *polyelectrolyte solution* of the same concentration. Finally, at higher Q, there is a shoulder at $d = 63$ Å and an oscillation at $h = 32$ Å.

The *surfactant scattering* is now as strong as the polymer scattering. It shows a first peak at a Q position that matches the polymer peak ($\xi = 141$ Å) and then a second peak at $d = 63$ Å. These features are reproduced in the polymer curve. Therefore the dissolved macromolecules and the surfactant micelles must be associated in the same structures. These features also resemble those found in solutions of *neutral macromolecules with bound surfactant micelles*.[16]

Additional information on the structures of these polymer−surfactant complexes may be obtained from the peak positions and from the variations of these positions with the composition of the solution. Figure 6 presents the surfactant scattering curves from samples made with a fixed surfactant concentration ($C_s = 0.015$) and various polymer concentrations (S/P = 0.3−1.0). All these curves show the two peaks described above. The peak at low Q shifts according to the polymer concentration. Figure 7 shows that the variation is a power law, $Q_{max} \sim \sqrt{C_p}$. This is the law expected for polyelectrolytes or any charged rodlike objects. Accordingly, this peak corresponds to a distance ξ between neighboring macromolecules that are loaded with charged surfactant micelles. A similar behavior was observed for PEO macromolecules loaded with SDS micelles.[16] The peak at high Q (corresponding to $d = 63$ Å) remains independent of the polymer concentration. Therefore it must correspond to an internal distance of the polymer−

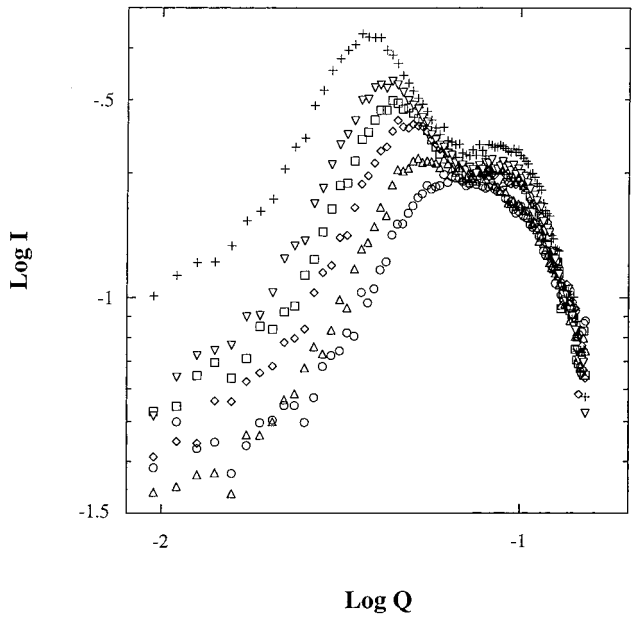

Figure 6. Scattering from surfactant in samples with fixed surfactant concentration (C_s = 0.015 g/mL) and varying S/P at T = 40 °C: (circles) S/P = 0.3 (turbid); (triangles) S/P = 0.4 (clear); (diamonds) S/P = 0.5 (clear); (squares) S/P = 0.6 (clear); (inverted triangles) S/P = 0.7 (clear); (crosses) S/P = 1 (clear).

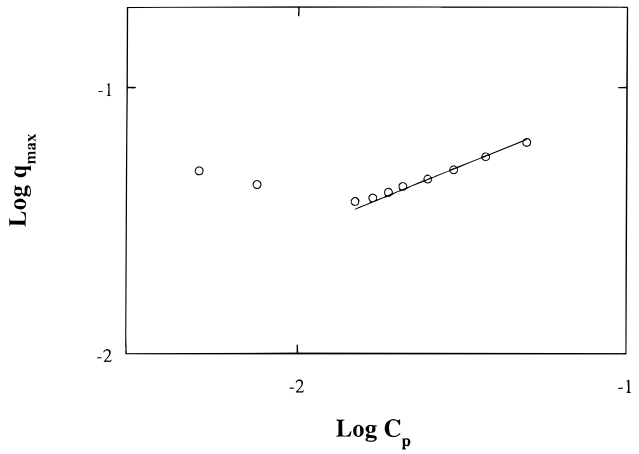

Figure 7. Positions of the peaks located at lower Q in the surfactant scattering curves of Figure 6, for various polymer concentrations (C_s = 0.015 g/mL, S/P = 0.3−2). The continuous line has a slope of 0.5.

surfactant complexes, which remains the same when the number of polymer−surfactant complexes is varied. Since the SDS concentration is above the critical aggregation concentration, the SDS molecules form micelles bound to the macromolecules, and this peak corresponds to a distance between micelles consecutively bound to a macromolecule.[16]

The two data points at C_p < 0.01 in Figure 7 correspond to samples with S/P > 1. Here, the two peaks in the surfactant curve are replaced by a single peak, as explained below.

S/P ≥ 2. These samples are clear solutions. The *polymer scattering* is essentially flat at low Q (Figure 8); a comparison with the spectra of samples made at lower S/P ratios confirms that the low Q depression has filled up. Therefore the repulsions between dissolved macromolecules must be screened at high S/P ratios. At higher Q values, corresponding to distances below the interpolymer distance ξ, the scattering curve decays as in the other samples. Thus, in samples made at large

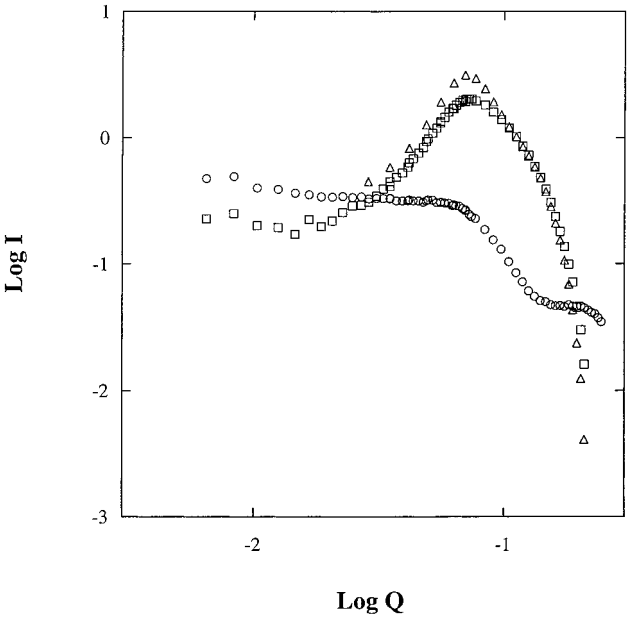

Figure 8. Scattering from samples with C_p = 0.03 g/mL and S/P = 2 at T = 40 °C (clear solution): (circles) scattering from polymer; (squares) scattering from surfactant; (triangles) scattering from surfactant in the absence of polymer.

S/P ratios, *the intramacromolecular correlations* are the same as in samples made at lower S/P, but the *intermacromolecular correlations* are screened. This screening must be caused by the large amount of excess surfactant, as explained below.

The *surfactant scattering* shows a depression followed by a single, intense peak. This spectrum is identical to the scattering from a micellar solution of SDS at the same concentration in the absence of polymer. In particular, the peak position matches the average intermicellar distance in pure SDS solutions. Thus, instead of having two intermicellar distances, as in samples made at lower S/P values, we now see a single one, which is not affected by the macromolecules. Therefore, at this high value of S/P, the surfactant peak that corresponds to the interchain distance ξ is swamped by the free intermicellar peak.

Temperature T = 20 °C. S/P = 0. This sample is a clear solution, as opposed to the phase separation observed at 40 °C. This difference is reflected in the intensity scattered by the polymer, which is much weaker. The scattering curve is shown in Figure 9. At low Q, it follows the Guinier law, eq 4, where I_0 is determined by the molar mass of individual macromolecules, and R_g is their radius of gyration. At higher Q values, the decay of the intensity follows a $Q^{-\alpha}$ power law; we find α = 1.7, which corresponds to the configurational statistics of swollen polymer coils in a good solvent.

S/P = 0.1 and 0.2. The scattering from the polymer in these samples is depressed as the surfactant concentration is increased (Figure 9). This depression indicates that the macromolecules repel each other. These repulsions originate from the electrical charges of the surfactant micelles that are bound to the macromolecules.

S/P = 0.5 and 1.0. The scattering curves of the polymer show a deeper depression at low Q, again from repulsions between surfactant-loaded macromolecules. This depression is followed by a peak corresponding to a distance between the polymer−surfactant complexes (Figure 10). The corresponding real space distances are

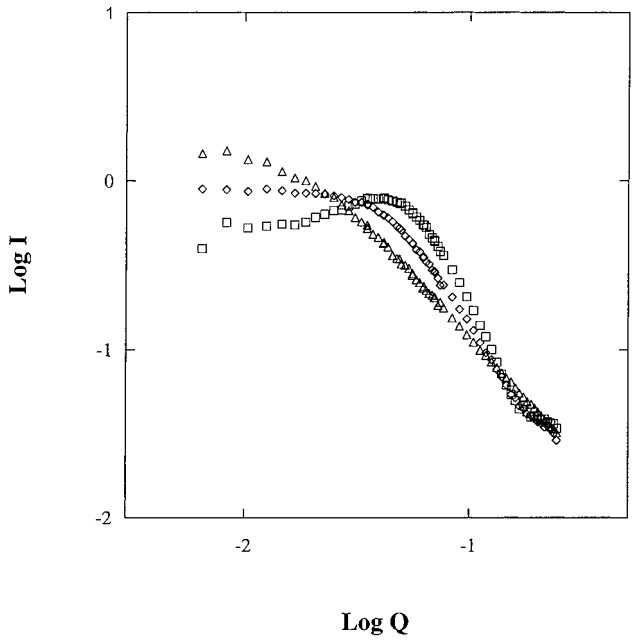

Figure 9. Scattering from polymer in samples with low S/P at $T = 20$ °C (all solutions are clear): (triangles) S/P = 0; (diamonds) S/P = 0.1; (squares) S/P = 0.2; (Compare with the scattering from samples at 40 °C, presented in Figure 2.)

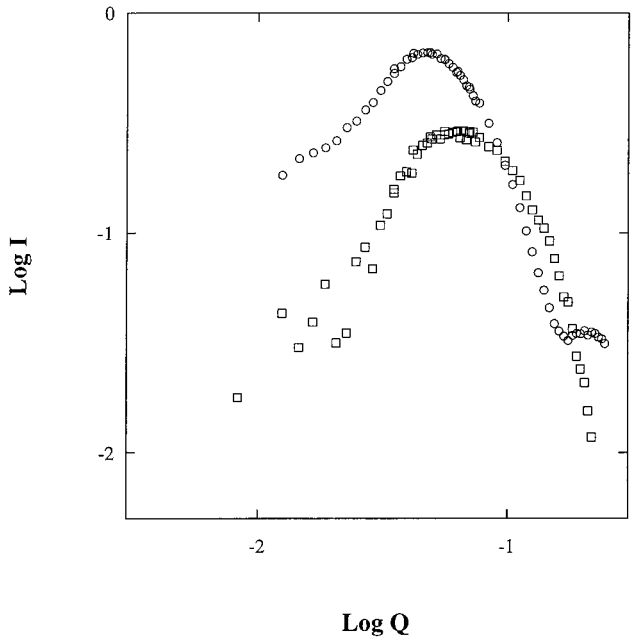

Figure 10. Scattering from samples with $C_p = 0.03$ g/mL and S/P = 0.5 at $T = 20$ °C (clear solution): (circles) scattering from polymer; (squares) scattering from surfactant. (Compare with scattering from sample at 40 °C, presented in Figure 5.)

slightly smaller compared to those obtained at 40 °C (for $R = 0.5$, $\xi = 131$ Å compared to 141 Å at 40 °C).

The surfactant scattering curves also show a depression followed by a broad peak (Figure 10). This peak is located between the positions of the two peaks observed in the scattering curves taken at 40 °C. Accordingly, the two distances ξ and d that were identified at 40 °C now appear to merge due to the shorter interchain distance ξ, as already observed in the polymer scattering. This indicates that the macromolecules are now more stretched. Conversely, the distance d corresponding to the intrachain surfactant distance is larger at 20 °C, indicating that consecutive micelles in a "necklace" are further apart, also because the macromolecules are more stretched. This is because water is a good solvent at 20 °C and the polymer chains are swollen: excluded volume interactions of the hydrated polymer segments together with the electrostatic repulsion of the micelles determine this distance. Indeed, the corresponding distance reported for the PEO−SDS system is around 80 Å[11,16] compared to 63 Å for the present system at 40 °C.

General Discussion

The aim of this work was to understand how surfactants transform the precipitation behavior of PNIPAM macromolecules at temperatures above the cloud point (or LCST). It was found that the transformations occur in 3 stages, according to the surfactant/polymer ratio, S/P. We start with the pure polymer−water system, which separates into a dense polymer phase and excess water, and we examine successively the structures of samples made at increasing surfactant/polymer ratios.

Temperature $T = 40$ °C. Very Low Surfactant/Polymer Ratios (S/P ≤ 0.1). In this range the precipitated polymer is fragmented into *colloidal particles*. These colloidal particles have already been observed by Pelton.[6,7] The average outer radius of these particles is around 200 Å with a high degree of polydispersity. Therefore they can be described as fragments of the dense polymer phase that separates out of water at temperatures above the LCST. The cause of this fragmentation is the presence of SDS. It may occur either as a result of equilibrium conditions or as a result of a nonequilibrium process.

We define as *equilibrium fragmentation* a situation where the dispersion of colloidal particles, with this average radius, is the state of lowest free energy of the system, in the same way as a dispersion of surfactant-covered oil droplets may be the state of lowest free energy of a microemulsion. This would imply that the colloidal particles would have zero interfacial tension, which would be a result of the adsorption of SDS. There is, in fact, just enough surface area on the colloidal particles to accommodate a monolayer of SDS. However, it is not obvious how the adsorption of SDS would cancel the surface tension of the particles.

We define as *nonequilibrium fragmentation* a process where the state of lowest free energy is made of two macroscopically separated phases, but SDS molecules bound to the colloidal particles prevent the formation of these phases. As the macromolecules are heated above the LCST, they dehydrate and collapse. For macromolecules of molar mass $M = 1.05 \times 10^6$ g/mol, a single collapsed macromolecule would form a globule with an outer radius of 70 Å. At surfactant/polymer ratios S/P ≤ 0.1, the number of available SDS molecules per macromolecule would be $n \leq 350$, which is not enough to fully cover the surface of the PNIPAM globule. Therefore these collapsed globules could aggregate until the surface/volume ratio of the resulting particles would be such that their surfaces would be entirely covered by SDS.[18]

At present we do not have results that would discriminate between these possibilities. In order to assess whether the colloidal particles represent an equilibrium or a nonequilibrium state of the system, it would be necessary to try to reach the same state by different routes, for instance, add SDS to pure precipitated PNIPAM at 40 °C or withdraw SDS from a PNIPAM + SDS solution at 40 °C.

Transition Region (S/P = 0.2 and 0.3). In this range the colloidal particles are dissolved by the added

SDS. For each particle, this occurs as a phase transition rather than a progressive phenomenon. Indeed, the polymer spectra show that dense particles coexist with dissolved macromolecules. The dense colloidal particles appear to be the same as those formed at lower S/P ratios. The dissolved macromolecules must be loaded with surfactant: indeed, the polymer spectra show depressions and peaks that can only be produced by repulsions between charged aggregates such as micelles (Figure 4). Remarkably, no intermediate states are found that would be either particles of reduced size or dissolved macromolecules loaded with less surfactant. This was shown in Figure 2, where the polymer scattering curves show almost the same curvature at low Q, corresponding to little variation in the colloidal particle radii, and in Figure 4, where the high-Q peak on the surfactant scattering curve corresponding to a distance d between micelles adsorbed consecutively on a macromolecule was already found at $d = 63$ Å and does not vary with surfactant to polymer ratio (Figure 6).

The observation of a constant distance d between micelles consecutively bound to a macromolecule can be explained as follows. A center to center distance $d = 63$ Å corresponds to a surface to surface distance of about 30 Å. This distance is determined by a balance of repulsions and attractions. The repulsions originate from electrical charges on the micellar surfaces; they become quite strong at short distances. The attractions originate from the adsorption of PNIPAM on micelles; at 40 °C, the macromolecules are insoluble in water, and therefore the adsorption free energy is quite high. As a result, the distance d can become neither shorter nor longer.

Thus, the coexistence of dense colloidal particles with necklaces that have a fixed linear density of micelles can be described either as an abrupt dissolution of the particles when SDS is added or as an abrupt collapse of the macromolecules when SDS is removed.

Intermediate Ratios (S/P = 0.4−1). In this range, the PNIPAM is completely dissolved by the added SDS. The organization of dissolved macromolecules and surfactant can be described as a solution of "necklaces", where each necklace is formed by one macromolecule and a large number of bound micelles.[11,16] The scattering curves show that the distance between necklaces ξ varies in the manner expected for charged rodlike objects (Figure 7); this confirms the "necklaces" picture. The scattering curves also show that the distance between consecutive micelles in a necklace, d, remains locked at $d = 63$ Å. This is a result of the competition between electrostatic repulsions and polymer attractions discussed above. However, in the range S/P = 0.1−1, the amount of surfactant per macromolecule is varied, yet the scattering curves do not show the presence of excess surfactant. Since the number of micelles per macromolecule is locked, it is likely that the variation in the amount of surfactant is accommodated by changes in the number of surfactant molecules in each micelle.

Excess Surfactant (S/P > 1). When the bound micelles have reached their maximum aggregation number, the necklaces can no longer bind more SDS. Therefore any additional SDS must remain as free micelles in the solution, coexisting with the necklaces. Because of this excess SDS, all micelles are now at the same distance, which explains the single peak in the surfactant scattering curve (Figure 8). Moreover, the macromolecules are now propagating among all these excess micelles, and no longer need to remain away from each other; this explains the loss of the repulsion between macromolecules in the polymer scattering curve (Figure 8). This saturation of the necklaces is quite similar to the stoichiometry observed in other polymer + surfactant systems.[11,16]

Temperature $T = 20$ °C. At this temperature, the PNIPAM is completely soluble. The scattering curves show that solutions of all compositions contain surfactant loaded macromolecules instead of forming colloidal polymer particles at low S/P ratios. Moreover, the structures of these necklaces differ from those found at 40 °C. Indeed, the surfactant scattering curves show a single peak only, instead of the two peaks observed at 40 °C. Accordingly, the distance ξ between necklaces is shorter than it was at 40 °C, and the distance d between consecutive micelles in a necklace is now longer than at 40 °C. Since the number of macromolecules is the same, the shorter ξ indicates that the macromolecules are more stretched out; indeed, the distance between macromolecules must vary as the inverse square root of their mass per unit length. The longer d indicates that the adsorption strength, which pulls micelles together in a necklace, is weaker than it was at 40 °C. Both effects are obvious consequences of the greater solubility of PNIPAM at 20 °C, which allows longer bridging sections between consecutive micelles. These looser "necklaces" are then entirely similar to those found in PEO + SDS solutions.[11,16]

The last distance, h, observed in the polymer scattering curves is comparable to the micellar diameter. This distance appears only in the presence of surfactants and is present at both temperatures. In addition, it is independent of the polymer concentration. Therefore, this distance is an intrachain feature closely associated to the manner in which the polymer and micelles bind together: it suggests that the macromolecules wrap around the micelles in loops that are also at the micellar diameter.

Conclusion

PNIPAM has potential applications as a thermosensitive switching device for aqueous systems. These applications are based on the polymer solubility in water at low temperatures and precipitation at higher temperatures. In this respect, the addition of SDS is interesting because it modifies the low-temperature and the high-temperature state of the polymer in water.

The low-temperature state is changed from a solution of independent macromolecules to a solution of "necklaces", where each macromolecule has collected a set of SDS micelles. Interestingly, no gel formation is observed, indicating that a micelle cannot be shared by two macromolecules.

The high-temperature state is changed, at low SDS concentrations, from a solid precipitate to a dispersion of colloidal polymer particles that are stabilized by surfactant, as in a latex dispersion. At higher SDS concentrations, the colloidal particles are converted to a solution of "necklaces", where the macromolecules are solubilized by the micellar surfaces. These necklaces are tighter than those formed at lower temperatures; still, they do not connect to each other, and therefore do not form gels.

These changes make the switching behavior of PNIPAM more versatile and easier to control than in the absence of surfactant. They also open the possibility of designing more complex behaviors with copolymers

that would have some sections with the same marginal solubility as PNIPAM and other sections that would remain swollen at all temperatures: at low levels of surfactants, the insoluble sections may collapse to form colloidal particles as in the PNIPAM case, and the soluble sections may provide interparticle connectivity and swelling.

Acknowledgment. This is a good moment for L.T.L. to thank J. Teixeira of LLB; his help on PAXE, and, more importantly, his support and encouragement in developing this project are much appreciated. We would also like to thank S. Egelhaaf for his assistance on D22 and P. Lixon for the characterization of the polymer.

References and Notes

(1) Wu, C.; Zhou, S. *Macromolecules* **1995**, *28*, 5388.
(2) Wu, C.; Zhou, S. *Macromolecules* **1997**, *30*, 574.
(3) Schild, H. G. *Prog. Polym. Sci.* **1992**, *17*, 163.
(4) Schild, H. G.; Tirrell, D. A. *Langmuir* **1991**, *7*, 665.
(5) Ricka, J.; Meewes, M.; Nyffenegger, R.; Binkert, Th. *Phys. Rev. Lett.* **1990**, *65*, 657.
(6) Wu, X. Y.; Pelton, R. H.; Tam, K. C.; Woods, D. R.; Hamielec, A. E. *J. Polym. Sci.: Part A: Polym. Chem.* **1993**, *31*, 957.
(7) Tam, K. C.; Wu, X. Y.; Pelton, R. H. *J. Polym. Sci.: Part A: Polym. Chem.* **1993**, *31*, 963.
(8) Meewes, M.; Ricka, J.; de Silva, M.; Nyffenegger, R.; Binkert, Th. *Macromolecules* **1991**, *24*, 5811.
(9) Heskins, M.; Guillet, J. E. *J. Macromol. Sci., Chem.* **1969**, *2*, 1441.
(10) Jacrot, B. *Rep. Prog. Phys.* **1976**, *39*, 911.
(11) Cabane, B.; Duplessix, R. *J. Phys. Fr.* **1982**, *43*, 1529.
(12) Cabane, B. In *Surfactants in Solution: New Methods of Investigation*; Zana, R., Ed.; Dekker: New York, 1986.
(13) Hayter, J. B.; Penfold, J. *J. Chem. Soc., Faraday Trans. 1* **1981**, *77*, 1851.
(14) Hayter, J. B.; Penfold, J. *Mol. Phys.* **1981**, *42*, 109.
(15) Kotlarchyk, M.; Chen, S. H. *J. Chem. Phys.* **1983**, *79*, 2461.
(16) Cabane, B.; Duplessix, R. *J. Phys. Fr.* **1987**, *48*, 651.
(17) Nierlich, M.; Williams, C. E.; Boue, F.; Cotton, J. P.; Daoud, M.; Farnoux, B.; Jannink, G.; Picot, C.; Moan, M.; Wolff, C.; Rinaudo, M.; de Gennes, P. G. *J. Phys. Fr.* **1979**, *40*, 701.
(18) Lannibois, H.; Hasmy, A.; Botet, R.; Aguerre Chariol, O.; Cabane, B. *J. Phys. II* **1997**, *7*, 319.

MA9704469